




Article

A Possible Role of Copernicus Sentinel-2 Data to Support Common Agricultural Policy Controls in Agriculture

Filippo Sarvia ¹, Elena Xausa ², Samuele De Petris ¹, Gianluca Cantamessa ²
and Enrico Borgogno-Mondino ^{1,*}

¹ Department of Agricultural, Forest and Food Sciences, University of Turin, L.go Braccini 2, 10095 Grugliasco, Italy; filippo.sarvia@unito.it (F.S.); samuele.depetris@unito.it (S.D.P.)

² Agenzia Regionale Piemontese per le Erogazioni in Agricoltura, Via Bogino 23, 10123 Torino, Italy; elena.xausa@arpea.piemonte.it (E.X.); gianluca.cantamessa@arpea.piemonte.it (G.C.)

* Correspondence: enrico.borgogno@unito.it

Abstract: Farmers that intend to access Common Agricultural Policy (CAP) contributions must submit an application to the territorially competent Paying Agencies (PA). Agencies are called to verify consistency of CAP contributions requirements through ground campaigns. Recently, EU regulation (N. 746/2018) proposed an alternative methodology to control CAP applications based on Earth Observation data. Accordingly, this work was aimed at designing and implementing a prototype of service based on Copernicus Sentinel-2 (S2) data for the classification of soybean, corn, wheat, rice, and meadow crops. The approach relies on the classification of S2 NDVI time-series (TS) by “user-friendly” supervised classification algorithms: Minimum Distance (MD) and Random Forest (RF). The study area was located in the Vercelli province (NW Italy), which represents a strategic agricultural area in the Piemonte region. Crop classes separability proved to be a key factor during the classification process. Confusion matrices were generated with respect to ground checks (GCs); they showed a high Overall Accuracy (>80%) for both MD and RF approaches. With respect to MD and RF, a new raster layer was generated (hereinafter called Controls Map layer), mapping four levels of classification occurrences, useful for administrative procedures required by PA. The Control Map layer highlighted that only the eight percent of CAP 2019 applications appeared to be critical in terms of consistency between farmers’ declarations and classification results. Only for these ones, a GC was warmly suggested, while the 12% must be desirable and the 80% was not required. This information alone suggested that the proposed methodology is able to optimize GCs, making possible to focus ground checks on a limited number of fields, thus determining an economic saving for PA and/or a more effective strategy of controls.

Keywords: common agricultural policy; service prototype development; crop monitoring; crop detection; random forest classification; minimum distance classification



Citation: Sarvia, F.; Xausa, E.; Petris, S.D.; Cantamessa, G.; Borgogno-Mondino, E. A Possible Role of Copernicus Sentinel-2 Data to Support Common Agricultural Policy Controls in Agriculture. *Agronomy* **2021**, *11*, 110. <https://doi.org/10.3390/agronomy11010110>

Received: 17 December 2020

Accepted: 5 January 2021

Published: 8 January 2021

Publisher’s Note: MDPI stays neutral with regard to jurisdictional claims in published maps and institutional affiliations.



Copyright: © 2021 by the authors. Licensee MDPI, Basel, Switzerland. This article is an open access article distributed under the terms and conditions of the Creative Commons Attribution (CC BY) license (<https://creativecommons.org/licenses/by/4.0/>).

1. Introduction

1.1. CAP and Contributions to Agriculture in the EU

The Common Agricultural Policy (CAP) represents the set of rules issued by the European Union (EU) for the regulation of the agricultural sector, with the aim of pursuing its harmonized development within all the Member States. CAP, as set out in Art. 39 of the Treaty on the Functioning of the European Union (TFEU), aims at increasing agricultural productivity [1], ensuring standards of living for the agricultural community, stabilizing markets and guaranteeing the availability of supplies, without neglecting environmental sustainability, food safety, and animal welfare [2,3].

CAP is founded by EAGF (European Agricultural Guarantee Fund) and EAFRD (European Agricultural Fund for Rural Development), which finance the first and second pillar, respectively, within a general strategy that supports the main actions in agriculture. Additionally, other national and regional investments are possible from each Member

Country, aimed at supporting peculiar and local interventions [4–6]. More specifically, CAP's first pillar, supported by the EAGF fund, concerns the Common Organization of Markets (CMO) supporting farmers with direct payments, that rewards actions favoring markets stabilization, increasing of agricultural production, environmental sustainability, and providing fair support to the life standard of farmers. EU delegates to Member States the following mandatory actions: (a) definition and application of the basic payment scheme; (b) definition and application of young farmers payment scheme (<40 years old that have been working as farmers for less than five years); (c) greening interventions, that guarantee additional payments per area for those farmers implementing practices that generate environmental benefits (e.g., crop diversification, maintenance of existing permanent grasslands, and ecological focus areas). Additionally, other direct payments can be activated voluntarily by the Member States: (a) contributions for areas showing natural constraints/less favored areas; (b) small farmers; (c) coupled payments; (d) redistributive payments for first hectares.

CAP second pillar, supported by EAFRD and regional/national funds, promotes sustainable rural development. In particular the objectives are: fostering agricultural competitiveness, ensuring sustainable management of natural resources, climate action, and development of rural economies and communities [7]. Member States (or their regions) define multi-annual rural development programs, personalized and divided into different measures, which must respond to EU rural development policy. Table 1 shows the prospectus of CAP funds addressed to Italy in the 2014–2020 period [8].

Table 1. Common Agricultural Policy (CAP) funding to Italy from 2014 to 2020 (billion euros) (Source: Ministry of Agricultural, Food and Forestry Policies).

Fund	European Union Funds	National Funds	Total	Annual Average
Direct Payments	27	0	27	3.8
Common Organization of Markets (CMO) wine, fruit, and vegetables	4	0	4	0.6
Rural development	10.5	10.5	21	3
Total	41.5	10.5	52	7.4

1.2. Types of CAP Controls

Farmers that intend to access CAP contributions must apply to the territorially competent Paying Agency. Payment claims must provide precise and updated information regarding areal consistency and structural features of farm. As required by Art. 17 of Reg. (EU) n. 809/2014 [9], applications must be based on geospatial data. GSAA (Geo Spatial Aid Application) describe farm parcels information through a GIS-based (geographic information system) approach and can be managed by paying agencies through the Integrated Management and Control System (IACS). IACS, additionally, allows unambiguous identification of agricultural parcels, connection to digital databases and execution of systematic checks [10]. GSAA contains information about land use and size of parcels and location of the (eventual) ecological focus areas. IACS is used by Paying Agencies in order to verify applications compliance with requirements and it relies on administrative (AC) and spot checks (SC). AC is performed on 100% of applications and aims to automatically detect formal faults through informatics tools. In particular, AC are called to verify compliance with eligibility criteria and maintenance of long-term commitments; compliance with deadlines for submitting payment claims; completeness of supplied documentation; absence of other financing quotes through other EU schemes. SC are generally performed with reference to five percent of applications with the aim of checking truthfulness of declared area size, verifying eligibility criteria, and testing compliance with envisaged commitments and obligations. SC are generally operated by photo-interpretation of high resolution satellite images and/or, in specific and rare cases, by direct ground checks (GCs).

1.3. Remote Sensing and CAP Controls

Crop monitoring by Earth Observation (EO) satellites is a possible alternative methodology to SC and it was recently proposed by EU Reg. No. 809/2014 Art. 40 bis amended by EU Reg. No. 746/2018. The Italian Agency for Payments in Agriculture (AGEA), that represents the national agency for CAP application in Italy, was the first one (2018) to test a satellite-based monitoring system during a pilot project involving the Province of Foggia (SE-Italy). It was aimed at checking applications related to the Basic Payment and Small Farmers scheme (Title III and V, respectively, of EU Regulation no. 1307/2013).

1.4. Study Goals

Within this context, in 2019, the Piemonte Agency for Payments in Agriculture (ARPEA), in collaboration with the Department of Agricultural, Forest and Food Sciences (DISAFA) of the University of Turin and the Aerospace Logistics Technology Engineering Company (ALTEC), activated its own experimental phase. The project was addressed to calibrate deductions from remote sensing to fit the specific local agricultural context, that appeared to be significantly different from the one where the previously mentioned national experience was run. The aim of this work was to design and develop a prototype service for crop classification based on multitemporal Copernicus Sentinel data. In particular, research outcomes were: (a) reduction of the overall costs for controls related to GCs and related administrative procedures; (b) minimization of subjectivity affecting the photo-interpretation process; (c) a timely update of irregular GSAA by farmers in consequence of warning coming from the system. Definitely, the project was intended to replace and/or integrate SC as required by EU regulations. Nevertheless, the possibility of classifying main crops over the whole regional territory can also be useful to resolve contradictions between public administration and farmers that arise in various stages of the administrative procedure. With these premises, a pilot area was selected within the Province of Vercelli.

2. Materials and Methods

2.1. Study Area

Piemonte Region (NW-Italy) consists of 8 Provinces, each of them with peculiar geomorphological and climatic characteristics, which determine different agricultural landscapes with different crop vocation. The study area (AOI) corresponds to the flat part of the Vercelli province (Figure 1). It is about 2081 km² and is entirely contained in a single Sentinel-2 (S2) tile. It is highly devoted to extensive agriculture with a prevalence of submerged crops (rice).

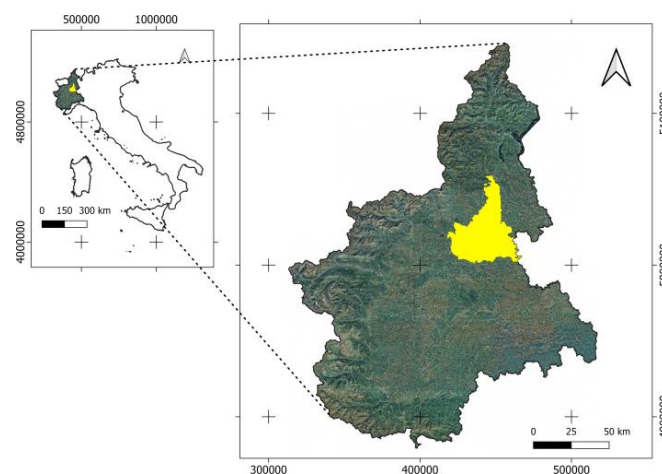


Figure 1. Study area (yellow) is located within the province of Vercelli in the Piemonte Region, NW Italy. (Reference system is WGS 84/UTM zone 32N, EPSG: 32632).

2.2. Monitored Crops and Related Agronomic Calendar

Currently, crop detection for AC is performed by photo-interpretation of aerial orthoimages with a time frequency of 3 years. Conversely, three VNIR (visible-NIR) high-resolution satellite image are photo-interpreted to support SC every year; in case of doubts, GCs are performed. Detection by satellite data is the expected (at least partially) alternative to this process. In this work, attention was paid to recognition of five crops: soybean, corn, wheat, rice, and meadow. The choice relies on requirements from the basic payment scheme (Title III of Reg. (EU) 1307/2013), from the optional coupled support, and from the payment for agricultural practices beneficial for climate and environment (Title IV).

In particular, soybeans and rice are eligible for receiving additional payments provided by the coupled support. For selected crops, correspondent agronomic calendars were available (Figure 2) and were used to support improve phenological interpretations.

Crops	Interventions on crops											
	Nov	Dec	Jan	Feb	Mar	Apr	May	Jun	Jul	Aug	Sep	Oct
Soy beans Cycle 240 - 290 gg							Sowing		Max Vegetation		Harvest	
Corn Cycle 90 - 150 gg						Sowing (grains)	Sowing (silage)		Max Vegetation		Harvest	
Wheat Cycle 250 - 290 gg	Sowing						Max Vegetation	Harvest				Sowing
Rice Cycle 180 - 230 gg							Sowing		Max Vegetation		Harvest	
Meadow Cycle 365 gg					Max Vegetation		Mowing	Mowing	Mowing		Mowing	

Figure 2. Example of the cultivation phases for the analyzed crops in the province of Vercelli.

2.3. Available Data

The following data were used for this study: (a) Copernicus Sentinel 2 data; (b) GSAA database for EU incentives under CAP 2019; (c) data from ground surveys carried out by ARPEA Piemonte technicians in the 2019 growing season.

2.3.1. Satellite Data

Availability of EO satellite images is currently large [11,12]. Nevertheless, not all data are suitable for agronomic applications. In particular, to detect and monitor crops, basic operational requirements are: (a) an adequate geometric resolution with respect to fields size; (b) high temporal resolution for phenological phases detection; (c) spectral bands sensitive to crop parameters (biomass, photosynthetic activity); (d) costs compatible with agronomic sector (possibly free of charge). The Sentinel 2 mission presents a nominal time resolution of 5 days (cloud cover dependent); images are supplied for free already calibrated in at-the-ground reflectance with a maximum geometric resolution of 10 m. These features make them certainly compatible with the purpose of this work. EU mission S2 is equipped with multispectral optical sensors capable of acquiring spectral bands in the range 400–2500 nm (from visible to medium infrared). S2 data are made available by the European Space Agency (ESA) through different web portals. The official one is the Sentinel Scientific Open Data Hub (ESA, <https://scihub.copernicus.eu/>). For this work, 53 S2 Level-2A images (tile 32TMR) were obtained covering AOI along the 2019 growing season. The single tile covers an area of $100 \times 100 \text{ km}^2$, is orthorectified in the WGS84 UTM reference system. Level 2A products are supplied in at-the-ground reflectance (Bottom of the Atmosphere, BOA) and, consequently, they can be immediately used for terrestrial applications [13]. Technical characteristics of S2 Multi Spectral Instrument (MSI) sensor are shown in Table 2.

Table 2. Sentinel-2 Multi Spectral Instrument Technical characteristics.

Bands (nm)	Geometric Resolution (m)
B1: 433–453	60
B2: 458–523	10
B3: 543–578	10
B4: 650–680	10
B5: 698–713	20
B6: 733–748	20
B7: 773–793	20
B8: 785–900	10
B8a: 855–875	20
B9: 935–955	60
B10: 1360–1390	60
B11: 1565–1655	20
B12: 2100–2280	20
Radiometric resolution: 12 bit	
Temporal resolution: 5 (10) days	

S2 data are supplied equipped of some auxiliary information. The most interesting one for this work was the SCL layer defining pixel quality according to a numerical coding as reported in Table 3.

Table 3. Coding of pixel assignment classes adopted in the “scene_classification” layer provided with Level 2A products.

Code	Description
0	No data
1	Saturated or Defective
2	Dark area pixels
3	Cloud shadows
4	Vegetation
5	Not vegetated
6	Water
7	Unclassified
8	Cloud Medium Probability
9	Cloud High Probability
10	Thin Cirrus
11	Snow

2.3.2. Farmers’ Geospatial Data Applications

GSAA dataset is currently not accessible to all users. For this work, it was provided by ARPEA in vector format for the 2019 season. GSAA contains basic information about crops and in particular the declared crop type (Table 4). About 210,000 GSAA were collected within AOI.

Table 4. Example data contained in Geo Spatial Aid Application (GSAA).

ID GSAA	Municipality	Field Area (ha)	Declared Cultivation	Products	ID of Farm Company
10115784	Vercelli	0.5	Rice	Beans, seeds, grains	1467
13248425	Vercelli	0.72	Meadow	Forage	1462
27757591	Vercelli	2.49	Rice	Beans, seeds, grains	1191
25860265	Vercelli	1.39	Corn	Beans, seeds, grains	1712
24675625	Vercelli	0.18	Soybean	Beans, seeds, grains	1560
22426581	Vercelli	4.43	Barley	Beans, seeds, grains	763

2.3.3. Ground Surveys

A ground campaign was performed by ARPEA according to GCs' standard in summer 2019 in order to validate remotely sensed deductions. GCs information were then georeferenced by Topcon GRS-1 (Topcon Positioning Italy Srl, Ancona, Italy) GNSS (Global Navigation Satellite System) receiver coupled with Mercury© (Mercury Systems, Inc., Andover, MN, USA) post-processing software [14]. During GCs, information about actual crop type was recorded. Moreover, some interviews were done to farmers to collect information about main agronomics operations (plowing, sowing, harvesting, mowing, flooding, and dry) they adopted. A total of 641 fields, covering about 1410 ha, were surveyed. Table 5 shows number and size of fields surveyed for each crop type.

Table 5. Size and number of surveyed plots per crop type.

Crops	Number of Fields Surveyed	Total Area of Fields Surveyed (ha)
Soy	89	120.74
Corn	187	77.11
Wheat	105	847.78
Rice	159	108.25
Meadows	101	257.32

2.4. Data Processing

The main conceptual steps of the proposed methodology are reported in Figure 3. Involved steps are deeply explained in the following sections.

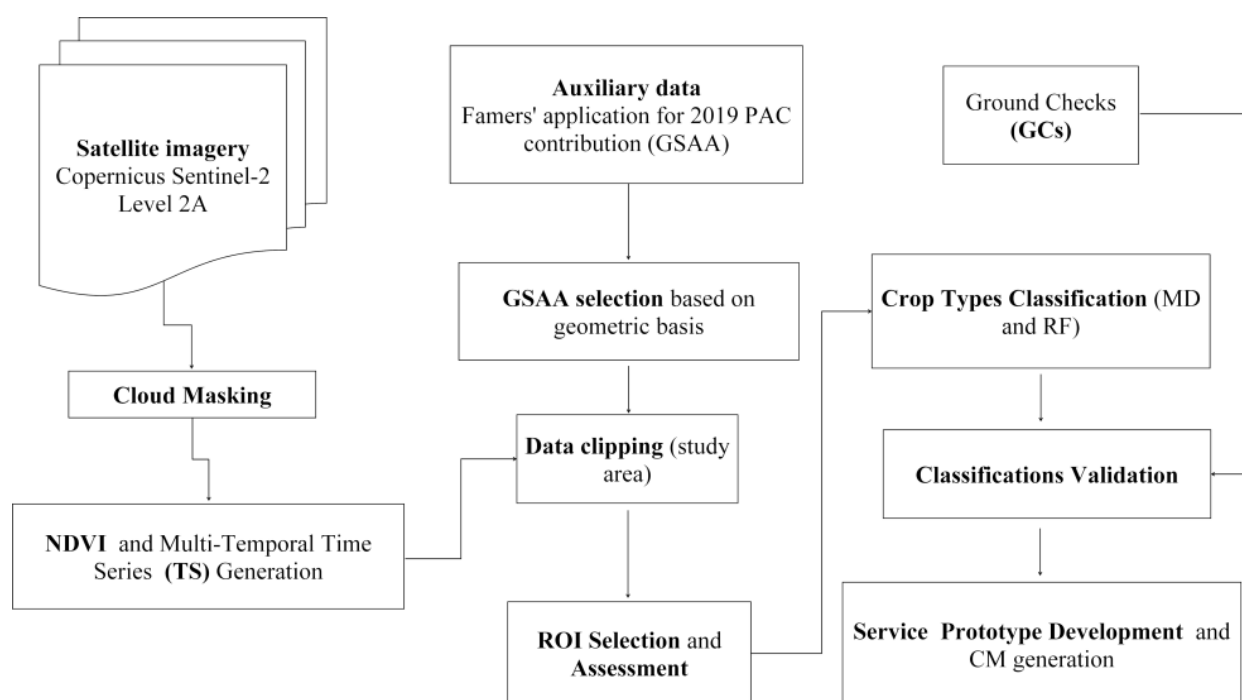


Figure 3. Main conceptual steps of the proposed methodology.

2.4.1. NDVI and Multi-Temporal Stack Generation

The Normalized Difference Vegetation Index (NDVI) is widely known in literature to be a spectral index able to retrieve information about vegetation [15–19], with special concern about phenology [20–22], ecosystems characterization [23], crop yield prediction [24,25], urban green areas and heat islands monitoring [26,27], tree vigor decline assessment [28,29], insurance strategies in agriculture [30–33]. In this work, NDVI was

assumed as phenology predictor and computed starting from the native S2 L2A imagery to compose a NDVI image time series covering the whole 2019 growing season. A similar image time series was generated with respect to the SCL layer and used to mask out bad observations during TS filtering and modelling. Filtering and modelling of NDVI temporal profiles were achieved at pixel level using a self-developed routine implemented in IDL v4.8 (Harris Geospatial Solutions, Inc., Broomfield, CO, USA) [34]. After bad observations removal, a spline-base interpolation (tensor value was set = 10) was performed in the time domain to regularize the local NDVI temporal profile. The resulting filtered and regularized NDVI time series assumed a nominal time frequency of 5 days [35,36]. Sixty-nine NDVI maps were finally obtained for the 2019 and stacked along a new time series (hereinafter called TS). TS was used to describe the temporal profile of each vegetated pixel in AOI and, consequently, its phenology (Figure 4).

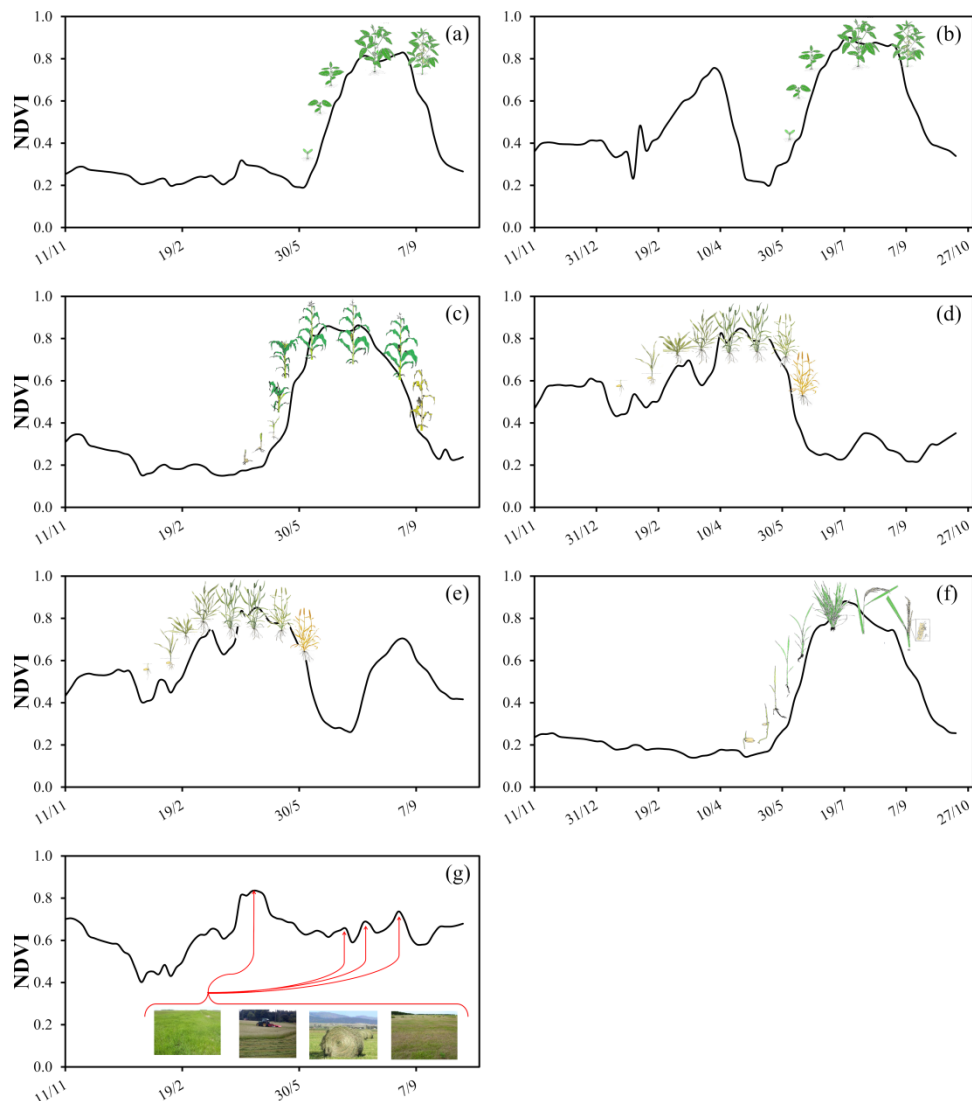


Figure 4. Examples of Normalized Difference Vegetation Index (NDVI) temporal profiles. They describe, at pixel level, NDVI evolution over time. (a) Soybean; (b) Soybean in succession with other crops; (c) Corn; (d) Wheat; (e) Wheat in succession with other crops; (f) Rice; (g) Meadow.

The basic assumption of this work was that NDVI temporal profile can be interpreted to recognize crops and related occurring management practices [37], especially when agronomic calendars are known. Several works adopted TS analysis in agriculture; for example Schreier [38] combined Landsat, S2 and MODIS data to map crop specific phenol-

ogy. Furthermore Gómez-Giráldez fused S2 and terrestrial photography to monitor grass phenology and hydrological dynamics [39]. According to ordinary agronomic uses, in this work, TS was generated with respect to the so called St. Martin's year (agronomic year) that starts/ends on the 11th November. This yearly time range is needed, in AOI, to correctly describe phenology of both "winter" (as autumn-winter cereals) and "summer" crops (as corn and rice). Such an approach was already proved to be effective in crop classification analysis [40].

2.4.2. Selection of Controllable Fields

Depending on the size and the shape of monitored fields, deductions can greatly vary in terms of reliability. In particular, the characterization of plot size and shape with respect to S2 geometrical resolution is fundamental. Not reliable measures can in fact occur while working with fields showing small size and/or a high shape anisotropy [41,42], mostly due to the so called mixed pixels whose spectral response results from the joint contribution of different type of covers. To take care about this issue, the Shape Index (SI, Equation (1)) and the area of GSAA polygons were computed by ordinary GIS tools available SAGA GIS 7.5 [43].

$$SI = \frac{P}{2\sqrt{\pi A}} \quad (1)$$

where P and A are the polygon perimeter and area, respectively [44]. All GSAA polygons having area less than 0.1 ha (about 3×3 pixels) and $SI \geq 3$ (very elongated shape) were masked out and labeled as "not controllable by satellite".

2.5. ROI Selection and Assessment

Preventively, NDVI value of each TS layer was averaged with respect to candidate polygons belonging to GSAA database. A supervised classification approach [45–47] based on the assessment of field average NDVI profile was selected as the most suitable one. With reference to focus crops, 151 regions of interest (ROI) were selected from GSAA and verified by querying and interpreting correspondent TS profiles. ROI distribution within AOI is shown in Figure 5.

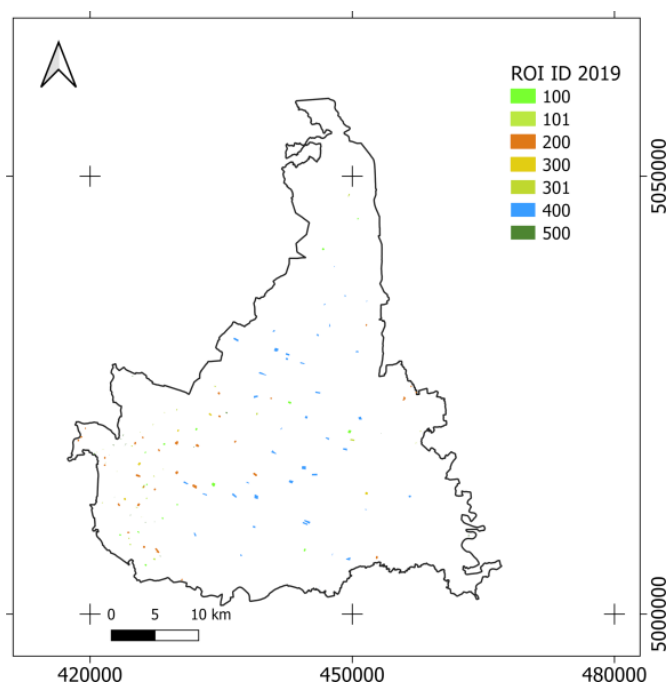


Figure 5. Regions of interest (ROI) distribution, code meaning is reported in Table 6 (Reference system is WGS 84/UTM zone 32N, EPSG: 32632).

Table 6. Characteristics of ROI.

Crop Class	ID ROI	ID Crop	#Plots	Area (ha)	Description
Soybean	100	1	16	26.57	Soya as the only crop for the entire agronomic year
	101		12	6.11	Soya in succession to a second crop
Corn	200	2	32	69.09	Corn as the only crop for the entire agronomic year
Wheat	300	3	14	11.54	Wheat as the only crop for the whole agronomic year
	301		21	32.22	Wheat grown on a second crop
Rice	400	4	40	289.37	Rice as the only crop for the whole agronomic year
Meadow	500	5	16	15.38	Meadow not alternated, as the only crop for the entire agronomic year, with some mowings
Total	-	-	151	450.29	-

TS profile interpretation was achieved by comparing it to available agronomic calendars. Wheat and soybean required to be separated in two different ROIs according to management type related to crop rotation [48,49]. Table 6 reports ROIs features: ROI and crop identifier (ID), sample size (n. of polygons and area), and class description. Figure 6 shows mean NDVI profiles (and standard deviation) of ROIs. To preventively explore ROIs separability, the pairwise Jeffries-Matusita test (JM) was run [50]. JM computes a parameter varying between 0 and 2, where 2 means complete separability of compared classes, 0 means no separability.

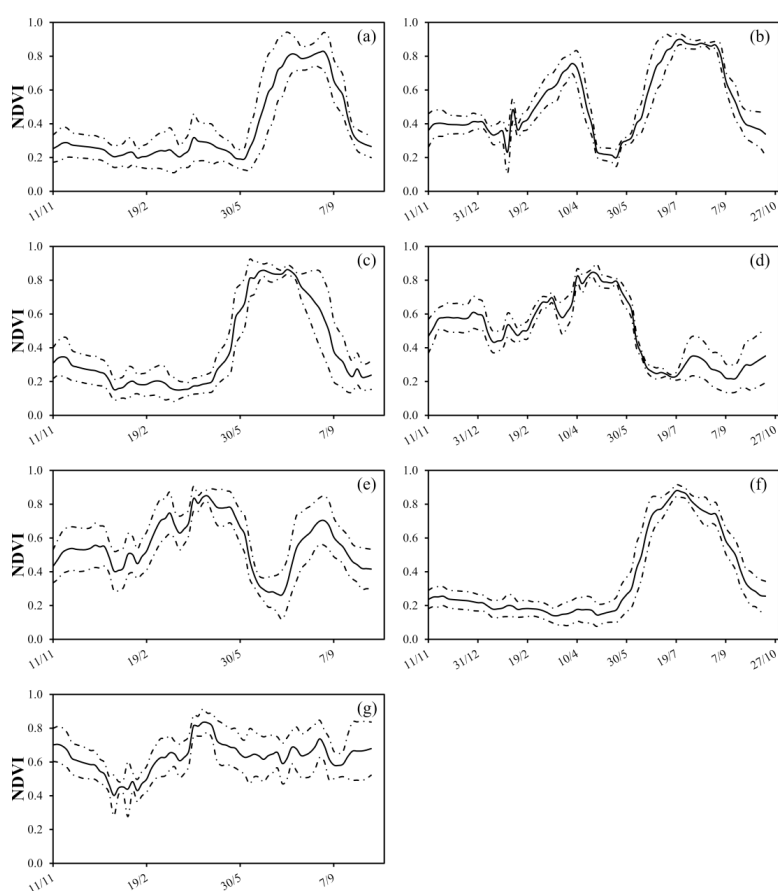


Figure 6. ROIs' average NDVI profiles throughout the 2019 season. Bold line represents mean profile; dotted lines are mean \pm standard deviation profiles. (a) Soybean-100; (b) Soybean-101; (c) Corn-200; (d) Wheat-300; (e) Wheat-301; (f) Rice-400; (g) Meadow-500.

2.6. Crop Type Classification

As previously mentioned, a plot-based classification approach was adopted in this work. Two algorithms were contemporarily used: Minimum Distance (MD) and Random Forest (RF) [51]. This choice relied on the consideration that crop type detection was expected to be ingested by ordinary workflows of CAP payment agencies. Consequently, the easier the approach, the easier the technological transfer. These algorithms areas are known to be fast and easy to be managed since they require the setting of few parameters and results are often reliable and satisfying. Conversely, they adopt different criteria to compare reference profiles (ROIs) with the local one. Consequently, an approach integrating two different answers to the same question retained a good choice for making results more robust. Many works in literature highlighted the performance and capability of these classifiers in the agricultural context [52,53]. Classifications were run using routines available in SAGA GIS 7.0.0.

2.6.1. Minimum Distance Classification

MD classifier is based on the computation of the Euclidean distance, in the iper-dimensional space defined by TS layers [54]. MD approach is certainly more effective when class dispersion is sufficiently low. MD admits the adoption of a distance threshold to accept or reject class assignation for the pixel/polygon. If this threshold is exceeded, pixel/polygon remains unclassified, i.e., it is not assigned to any of the classes. For this work, the distance threshold value was set to 1.3 points of NDVI.

2.6.2. Random Forest Classification

RF is a type of supervised machine learning algorithm based on multiple prediction models. Each model used by RF forecasting is usually a decision tree. This means that a RF combines many decision trees in a single model. Individually, the forecasts made by individual decision trees may not be accurate, but combined together, forecasts will be averagely closer to the true result. RF algorithm can be used for both regression and classification problems [55]. The use of RF in remote sensing in order to map different areas is widely discussed in the literature [56–59]. For this work, RF was run setting a number of trees equal to 10 and a number of training samples equal to 5000 pixels. RF design was decided with reference to some “unstructured” repeated trials. The best performing configuration, in terms of kappa coefficient value (K), was selected out of the RF run trials. Authors did not deepen further this issue since RF parameters selection is expected to be set up time by time when the classifier is run. Consequently, no general indication can be given at this point.

2.7. Classifications Accuracy Assessment

MD and RF classification were tested with respect to GCs in order to assess classification accuracy. In total, 664 GCs were used to generate the confusion matrices and compute performance parameters: overall accuracy (OA), user’s and producer’s class accuracy (UA and PA) and K were calculated [60].

2.8. Service Prototype Development

Classifications produced by MD and RF algorithms were integrated in a prototype system that could be used to verify truthfulness of GSAA. Initially, a spatial join was performed to transfer MD and RF class codes to GSAA attribute table. Based on this new dataset, hereinafter called controls map (CM), the following conditions were tested and a new code recorded in a further attribute table field (Table 7).

Table 7. Tested conditions and actions that the control system operates with respect to Minimum Distance (MD) and Random Forest (RF) classification results.

Assigned CM Code	Tested Condition	Action
1	Class assignment from MD and RF are both concordant to GSAA	No ground survey is needed
2	GSAA is equal to at least one classification	No ground survey is needed
3	Class assignment from MD and RF are different and both discordant with GSAA	A ground survey is suggested
4	Class assignment from MD and RF are equal but discordant with GSAA	A ground survey is needed

For each CM code, a specific administrative procedure is expected, involving (or not) GCs, depending on resulting priority. This prototypal methodology would allow paying agencies to proceed with PAC contributions payment and improving irregularities detection. Materials and Methods should be described with sufficient details to allow others to replicate and build on published results. Please note that publication of your manuscript implicates that you must make all materials, data, computer code, and protocols associated with the publication available to readers. Please disclose at the submission stage any restrictions on the availability of materials or information. New methods and protocols should be described in detail while well-established methods can be briefly described and appropriately cited.

Research manuscripts reporting large datasets that are deposited in a publicly available database should specify where the data have been deposited and provide the relevant accession numbers. If the accession numbers have not yet been obtained at the time of submission, please state that they will be provided during review. They must be provided prior to publication.

Interventionary studies involving animals or humans, and other studies requiring ethical approval must list the authority that provided approval and the corresponding ethical approval code.

3. Results and Discussions

3.1. Selection of Controllable Fields

GSAA data were filtered according to the above-mentioned geometric criteria involving SI and area parameters of fields. Only 22% (47,576 out of 208,675 starting) of the fields showed to satisfy geometric requirements to make them suitable to be controlled by S2 data. While in terms of surface area there is not a large decrease, from 115,647 ha to 85,854 ha (about 74% of the total). The huge reduction of controllable fields was mainly related to the peculiar fragmentation of the Italian agricultural landscape made of many small properties with highly anisotropic geometries. These fields were considered not reliable and have a poor impact on PAC contributions; therefore were masked out from all subsequently steps.

3.2. ROI Selection and Assessment

ROI separability assessment was performed according to JM and results are shown in Table 8. In general, low JM values, never exceeding 0.9, were found. This could be related to the frequency distribution of NDVI values along TS. It can be noted that many ROI profiles (Figure 6) contain observations with low NDVI values occurring when no active vegetation is present (winter or before the development/sowing of crops). This period, if included in the profile during the classification process, could make classes more similar, being possibly related to bare soil condition preceding vegetation growth.

Table 8. Test separability of ROI with JM, low values are underlined (JM low values between summer crops in red and JM low values between multi-modal TS profiles in blue).

ROI ID 2019	100	101	200	300	301	400	500
100		0.33	<u>0.10</u>	0.29	0.52	<u>0.10</u>	0.85
101			0.30	<u>0.09</u>	<u>0.24</u>	0.36	0.61
200				0.29	0.51	<u>0.06</u>	0.82
300					0.25	0.34	0.64
301						0.56	0.43
400							0.86
500							

In spite of this, JM test values can be used to explore class to class similarity. Table 8 shows that low values concern comparison between summer crops (in red), that necessarily present a similar phenology. For all of them, biomass is expected to be maximum in July–August and the growing season duration is similar as supported by their agronomic calendars (Figure 2). Wheat (winter crop) and soybeans (summer crop) show, expectably, low JM values: this was found to be majorly due to the succession of crops (a summer crop following a winter one) that, in many cases, is the ordinary field management strategy. This determines a multi-modal TS profiles that introduces noise when trying to use the NDVI profile of the whole season to separate crops. (Table 8 blue color). A higher separability was, instead, found between meadow and other classes.

3.3. ROI Selection and Assessment

Results of MD and RF classification are shown in Figure 7. Area size and number of classified fields are reported in Table 9 for all the classes. Although number and area size of plots were the same for both the classifications, MD classification was run setting a distance threshold that labeled as unclassified about 11,000 plots (about 19,500 ha). Rice resulted the main crop type in AOI for both MD and RF.

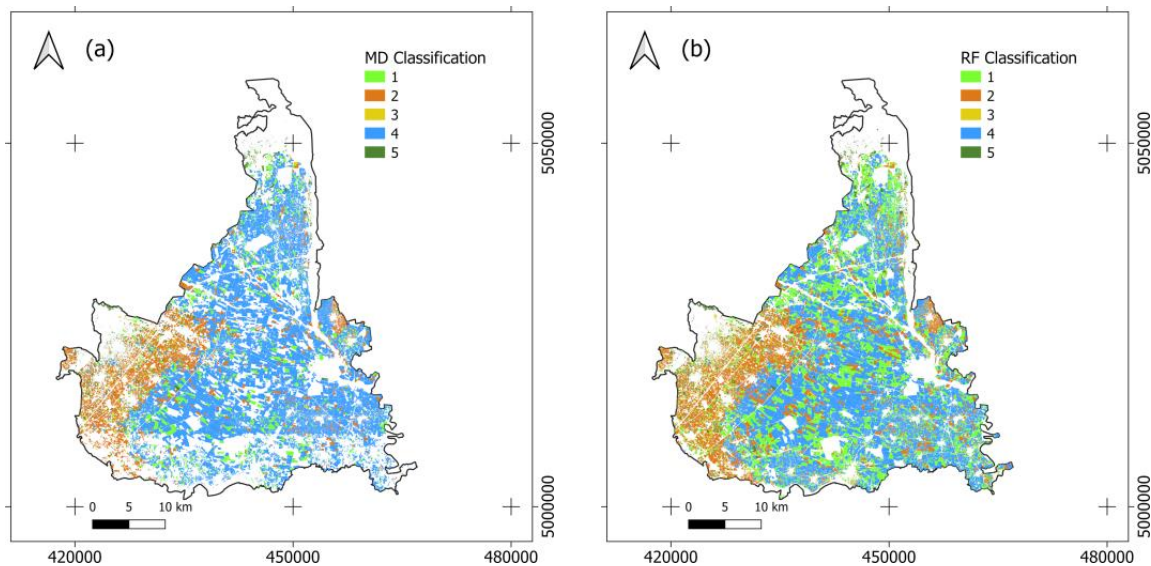


Figure 7. (a) MD Classification, (b) RF Classification. Code meaning is reported in Table 9 (Reference system is WGS 84/UTM zone 32N, EPSG: 32632).

Table 9. Test separability of ROI with Jeffries-Matusita test (JM).

Crop Classes	MD Classification		RF Classification	
	Number of Plots	Class Area (ha)	Number of Plots	Class Area (ha)
1	4180	7840.55	12,934	23,181.91
2	7683	11,337.21	11,004	17,418.45
3	655	786.39	1687	2086.42
4	21,446	44,441.33	19,063	40,444.23
5	2251	1768.32	2888	2552.56

3.4. Classification Accuracy Assessment

Classifications accuracy was tested with respect to GCs and the correspondent confusion computed (Tables 10–12). In general, it can be noted that: OA and K were high for both MD and RF (>80% and >0.70, respectively); user's class accuracy (UA) and producer's class accuracy (PA) for corn, rice, and meadow were high (>70%); soybean and wheat showed the lowest UA and PA values for both classifications (Table 12). This was already suggested by the JM test that highlighted a very low separability between these two classes, possibly due to the bi-modal NDVI profile characterizing many winter wheat fields, where a second crop is often planted after the yield. Soybean and rice, similarly, showed a high commission that could be related to their similar phenology. For these crops year periods when vegetation is not active seems to majorly affect classification commission. Similar results were obtained by Konduri [61] while classifying a large area in USA using multi-temporal MODIS (Moderate Resolution Imaging Spectroradiometer) data: resulting UA and PA values ranged from 40% to 60% for corn, wheat, soybean, and rice. Similarly, Belgiu [62] found comparable UA and PA values for corn, wheat, rice, and meadow in different study areas (USA, Romania, and Italy) basing classification on RF and S2 data. Additionally, the highly fragmented and varying Italian agricultural context, aiming at maximizing specificity and quality of products, certainly increase phenological differences also within the same crop class; this makes more probable that specific groups of the same class appear majorly similar to specific groups of another crop class. Some improvement of classification results can certainly come from the adoption of machine learning/artificial intelligence algorithms supported by additional discriminants like field geometrical and textural features, topographic parameters, and other spectral indices [63,64]. Nevertheless, the choice of basing the proposed procedure on simple, controllable, and "user-friendly" classification algorithms, still remains strategic in the present technological transfer context. In fact, in too many cases, technicians from stakeholders do not still possess remote sensing skills and a simplified approach to make them closer to this new approach is mandatory.

Table 10. Confusion matrix of AOI performed by MD classification.

Crop Codes	MD Classification					Total	
	1	2	3	4	5		
Classification	1	5961	591	837	5766	60	13,215
	2	2542	20,665	2101	15	527	25,850
	3	11	48	695	0	174	928
	4	1625	4041	1040	75,516	1596	83,818
	5	213	285	2468	30	9043	12,039
Total	10,352	25,630	7141	81,327	11,400	135,850	

Table 11. Confusion matrix of AOI performed by RF classification.

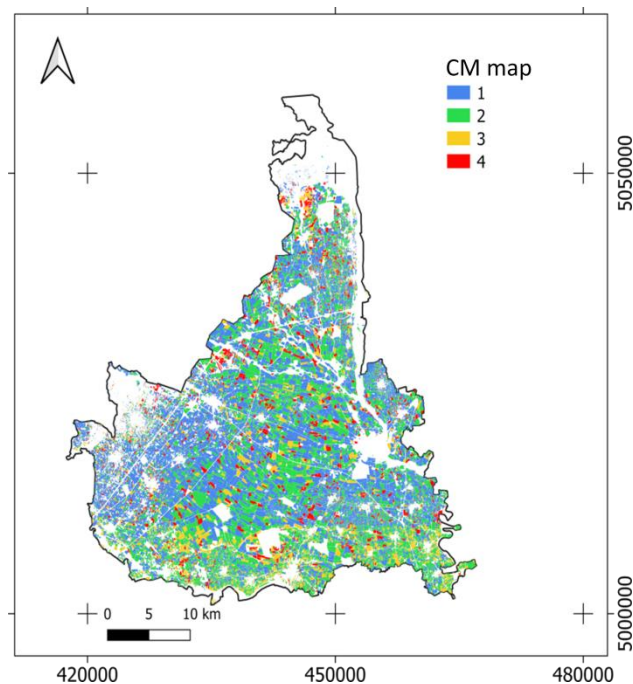
Crop Codes		RF Classification					Total
		1	2	Reference 3	4	5	
Classification	1	6362	108	1406	6658	60	14,594
	2	1394	22,763	694	4922	1463	31,236
	3	50	83	4878	5	596	5612
	4	2436	1636	47	71,191	16	75,326
	5	199	167	283	24	9292	9965
Total		10,441	24,757	7308	82,800	11,427	136,733

Table 12. Test separability of ROI with JM.

Crop Codes	MD Classification		RF Classification	
	UA	PA	UA	PA
1	45.11	57.58	43.59	60.93
2	79.94	80.63	72.87	91.95
3	74.89	9.73	86.92	66.75
4	90.10	92.85	94.51	85.98
5	75.11	79.32	93.25	81.32
OA	82.36		83.73	
K	0.70		0.73	

3.5. Service Prototype Development

CM layer (Figure 8), equipped with codes ideally activating ARPEA procedures for controls about truthfulness of GSAA, certainly represents an improving tool of present situation. In particular, it makes possible to extend preliminary controls to the 22% in AOI and define a priority of field campaigns. CM statistics for AOI are shown in Figure 9 with reference to monitored crops.

**Figure 8.** Controls map (CM). Code meaning is reported in Table 9. (Reference system is WGS 84/UTM zone 32N, EPSG: 32632).

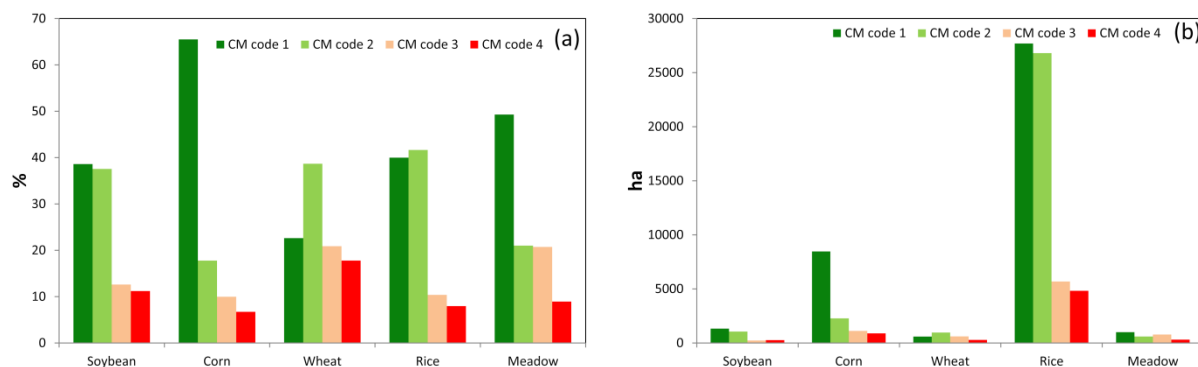


Figure 9. (a) CM code for each crops analyzed (%); (b) CM code for each crops analyzed in terms of surface (ha). Code meaning is reported in Table 9.

Figure 9 shows that 38,164, corresponding to 80% out of the total controlled fields, (22% of GSAA after shape/size filtering) seemed to not require GCs (CM code 1–2); 3964 GSAA (8% of controlled fields) appeared to require GCs (CM code 4). For 5448 fields (12% of controlled fields—CM code 3), MD, RF, and GSAA were not concordant with each other: deductions about these fields have to be considered unreliable making desirable (not mandatory) GCs. In terms of surface, Figure 9 shows that over 70,000 ha seemed to not require GCs (CM code 1–2); over 6500 ha appeared to require GCs (CM code 4); and for about 8000 ha (CM code 3), was suggested GCs. Summarizing, one can say that: (a) the procedure was able to test 22% of GSAA fields; (b) a reliable check (codes 1, 2, 4) was obtained for 88% of selected fields corresponding to about 19% of GSAA fields; (c) no reliable information concerned the 12% of selected fields corresponding to the 2.6% of GSAA fields. These could be reasonably included in the 5% of GSAA fields that are ordinarily controlled by ground campaigns, making selection more focused than previously. With respect to expectations from ARPEA, this approach still has a limit related to the need of using TS covering the entire growing season. This determines that classification results can be made available only at the end of the agronomical year (mid of October), making GCs impossible to be operated when crops have not still been harvested.

3.6. Future Developments

Future developments of this work will be certainly addressed to improve present classifications results. The joint adoption of many spectral indices, the integration of Sentinel 2 and Sentinel 1 data and the collection of additional structured agronomic parameters (e.g., Leaf Area Index, Growing Degree Day) area certainly need to be considered.

Moreover, some tests will be addressed to investigate if crop detection can be accurately obtained also before the end of the growing season by progressively shortening the sequence of NDVI observations. In this case, a time threshold should be identified and tested against time deadlines of administrative procedures of CAP controls to, eventually, make possible an early warning to farmers to correct their declarations.

3.7. Discussions

Farmers that intend to access CAP contributions must apply to the territorially competent Paying Agency through GSAA, a GIS-based procedure that contains information about land use and size of parcels and location of the (eventual) ecological focus areas. Paying Agencies are called to verify GSAA compliance with requirements through AC and SC. SC, in particular, are generally performed with reference to five percent of applications to verify truthfulness of declared crop type and areas, compliance of eligibility criteria, and envisaging of commitments and obligations. SC are presently operated by photo-interpretation of high-resolution satellite images and/or, in specific and rare cases, by direct ground checks (GCs). An important step, too often neglected, is the a-priori selection of those GSAA fields that can be reasonably controlled by satellite (i.e., showing

specific shape and size features). In AOI, only the 22% of fields proved to be compliant with shape/size requirements. While in terms of surface area, there is not a large decrease (about 74% of the total). As far as separability of crop classes, based on NDVI temporal profiles was concerned, it proved to be a key and limiting factor. Confusion matrices, built with respect to ground controls, showed an OA > 80% for both MD and RF. Commission and omission errors were not negligible, suggesting that some crops express similar phenological behaviors. Rice, soybean, and corn demonstrated to be poorly separable (JM < 0.10). Unexpectedly, wheat and soybean showed a low degree of separability and highlighted that some classification problems were due to winter crop-related practices where two successive crops are coupled along the year in the same field (bi-modal NDVI temporal profile). In spite of these improvable situations, meadow, rice, corn, and wheat classes proved to be reliably detectable (UA > 70%). From an operational point of view, the choice of coupling two classifiers (MD and RF) within the same procedure made possible to integrate correspondent results to generate the CM layer. The latter can be interpreted as a technical tool supporting the administrative process by ARPEA where, for each GSAA field suitable to be controlled by satellite, a code is assigned suggesting the administrative procedure to adopt during controls. In AOI, according to CM, the eight percent of PAC 2019 applications for fields suitable to be controlled by satellite (22% of the total), were recognized as requiring GCs, since detected class by remote sensing was different from the declared one; conversely, the 80% proved to be consistent with GSAA applications and, consequently, no GC was required. The remaining 12% referred to unreliable detection.

4. Conclusions

In this work, a prototype service was proposed aimed at supporting controls by institutional players (e.g., ARPEA) about farmers' EU CAP applications. This work was solicited by the Piemonte Agency for Payments in Agriculture (ARPEA) to support SC with special concern about five crops: soybean, corn, wheat, rice, and meadow. The proposed procedure, currently, represents one of the first institutional satellite-based workflows in the EU context. The procedure relies on NDVI time series from Copernicus Sentinel 2 data, assuming temporal profiles of NDVI as descriptors of crop phenology capable of discriminating crops through a classification process. In this work, NDVI profile classification was operated by coupled supervised classifiers that ensured easy use by unskilled users: Minimum Distance and Random Forest, both operating in the time domain of NDVI temporal profiles (OA < 80% for both algorithms). AOI was selected within the agriculture-devoted province of Vercelli (Piemonte Region), where a heterogeneous richness of crops was present, included the above mentioned five ones. In spite of this preliminary, but institutionally supported, experience, the proposed prototypal service proved to be able to optimize GCs, ranking, and mapping the priority of controls, thus allowing economic savings (over 70,000 ha, about 83% of monitorable fields, do not seem to require GCs). It is worth noting that, until 2016, only the five percent of GSAA were controlled according to a random selection. Conversely, the proposed procedure makes now possible to control all "suitable" GSAA and move field selection from a random to a focused and ranked sampling. Nevertheless, the reliability of deductions strictly depends on ROI quality and specificity where agronomic skills are basic. Consequently, the adoption of this tool within administrative workflows will have to take carefully into account that reliable data and should feed the system concerning training set to adopt during classification and that, the training set has to be updated annually.

Author Contributions: Conceptualization, F.S., E.X., and E.B.-M.; methodology, F.S. and E.B.-M.; software, F.S. and E.B.-M.; validation, F.S., E.X., and S.D.P.; formal analysis, F.S. and E.X.; investigation, F.S. and E.X.; resources, F.S., E.X., and G.C.; data curation, F.S. and E.X.; writing—original draft preparation, F.S., E.X., and S.D.P.; writing—review and editing, F.S., S.D.P., and E.B.-M.; visualization, F.S.; supervision, E.B.-M. and G.C.; project administration, E.B.-M. All authors have read and agreed to the published version of the manuscript.

Funding: This research received no external funding.

Institutional Review Board Statement: Not applicable.

Informed Consent Statement: Informed consent was obtained from all subjects involved in the study.

Data Availability Statement: Data sharing not applicable.

Acknowledgments: We would like to thank Chiara Leuzzi, Ruben De March, Angelo Fabio Mulone and Rosario Messineo, technicians by the Aerospace Logistics Technology Engineering Company (Altec), who worked together with DISAFA and ARPEA on this project pursuing classification with machine learning algorithms.

Conflicts of Interest: The authors declare no conflict of interest.

References

- Geiger, R.; Kotzur, M.; Khan, D.E. *European Union Treaties*; Hart Publishing: Oxford, UK, 2015.
- Fennell, R. The common agricultural policy: Continuity and change. In *OUP Cat*; Oxford University Press: Hong Kong, China, 1997.
- Shucksmith, M.; Thomson, K.J.; Roberts, D. *The CAP and the Regions: The Territorial Impact of the Common Agricultural Policy*; CABI Publishing: Wallingford, UK, 2005.
- Regulation, C. No 1257/1999 on Rural Development Support by Means of the European Agricultural Guarantee Fund (EAGGF). *J. Rural Stud.* **1999**, *23*, 416–429.
- Häring, A.; Dabbert, S.; Aurbacher, J.; Bichler, B.; Eichert, C.; Gambelli, D.; Zanolli, R. *Organic Farming and Measures for European Agricultural Policy*; Universität Hohenheim: Stuttgart, Germany, 2004.
- Cafiero, C.; Capitanio, F.; Cioffi, A.; Coppola, A. Risk and Crisis Management in the Reformed European Agricultural Policy. *Can. J. Agric. Econ. Can. Agroecon.* **2007**, *55*, 419–441. [[CrossRef](#)]
- Zarco-Tejada, P.J.; Hubbard, N.; Loudjani, P. Precision agriculture: An opportunity for EU farmers—Potential support with the CAP 2014–2020. *Joint Res. Centre Eur. Comm.* **2014**, *9*, 1339.
- Bonfiglio, A.; Henke, R.; Pierangeli, F.; D’Andrea, M.R.P. Direct Payments and Competitiveness. Assessing Redistributive Effects of Internal Convergence in Italy. *Agric. Food Policy* **2018**. [[CrossRef](#)]
- Reg. EU No. 809/2014 of the European Parliament and Council with Regard to the Integrated Administration and Control System, Rural Development Measures and Cross Compliance, EU. *Int. J. Remote Sens.* **2014**, *40*, 7272–7286.
- Campinas, M.; Rosa, M.J. Assessing PAC contribution to the NOM fouling control in PAC/UF systems. *Water Res.* **2010**, *44*, 1636–1644. [[CrossRef](#)] [[PubMed](#)]
- Defries, R.S.; Townshend, J.R.G. Global land cover characterization from satellite data: From research to operational implementation? GCTE/LUCC Research Review. *Glob. Ecol. Biogeogr.* **1999**, *8*, 367–379. [[CrossRef](#)]
- Justice, C.O.; Townshend, J.R.G.; Holben, B.N.; Tucker, E.C. Analysis of the phenology of global vegetation using meteorological satellite data. *Int. J. Remote Sens.* **1985**, *6*, 1271–1318. [[CrossRef](#)]
- Sentinel, E.S.A. *User Handbook*; ESA Standard Document; European Space Agency: Paris, France, 2015; p. 64.
- Hodgson, M.E. On the accuracy of low-cost dual-frequency GNSS network receivers and reference data. *GIScience Remote Sens.* **2020**, *57*, 907–923. [[CrossRef](#)]
- Leprieux, C.; Verstraete, M.M.; Pinty, B. Evaluation of the performance of various vegetation indices to retrieve vegetation cover from AVHRR data. *Remote Sens. Rev.* **1994**, *10*, 265–284. [[CrossRef](#)]
- Jiang, Z.; Huete, A.; Chen, J.; Chen, Y.; Li, J.; Yan, G.; Zhang, X. Analysis of NDVI and scaled difference vegetation index retrievals of vegetation fraction. *Remote Sens. Environ.* **2006**, *101*, 366–378. [[CrossRef](#)]
- Jönsson, P.; Eklundh, L. Seasonality extraction by function fitting to time-series of satellite sensor data. *IEEE Trans. Geosci. Remote Sens.* **2002**, *40*, 1824–1832. [[CrossRef](#)]
- Johnson, L.F.; Trout, T.J. Satellite NDVI Assisted Monitoring of Vegetable Crop Evapotranspiration in California’s San Joaquin Valley. *Remote Sens.* **2012**, *4*, 439–455. [[CrossRef](#)]
- Borgogno-Mondino, E.; Lessio, A.; Gomasasca, M.A. A fast operative method for NDVI uncertainty estimation and its role in vegetation analysis. *Eur. J. Remote Sens.* **2016**, *49*, 137–156. [[CrossRef](#)]
- Usman, M.; Liedl, R.; Shahid, M.A.; Abbas, A. Land use/land cover classification and its change detection using multi-temporal MODIS NDVI data. *J. Geogr. Sci.* **2015**, *25*, 1479–1506. [[CrossRef](#)]
- Pan, Z.; Huang, J.; Zhou, Q.; Wang, L.; Cheng, Y.; Zhang, H.; Blackburn, G.A.; Yan, J.; Liu, J. Mapping crop phenology using NDVI time-series derived from HJ-1 A/B data. *Int. J. Appl. Earth Obs. Geoinform.* **2015**, *34*, 188–197. [[CrossRef](#)]
- Wardlow, B.D.; Egbert, S.L. Large-area crop mapping using time-series MODIS 250 m NDVI data: An assessment for the U.S. Central Great Plains. *Remote Sens. Environ.* **2008**, *112*, 1096–1116. [[CrossRef](#)]

23. Orusa, T.; Orusa, R.; Viani, A.; Carella, E.; Borgogno-Mondino, E. Geomatics and EO Data to Support Wildlife Diseases Assessment at Landscape Level: A Pilot Experience to Map Infectious Keratoconjunctivitis in Chamois and Phenological Trends in Aosta Valley (NW Italy). *Remote Sens.* **2020**, *12*, 3542. [[CrossRef](#)]
24. Zambrano, F.; Vrieling, A.; Nelson, A.; Meroni, M.; Tadesse, T. Prediction of drought-induced reduction of agricultural productivity in Chile from MODIS, rainfall estimates, and climate oscillation indices. *Remote Sens. Environ.* **2018**, *219*, 15–30. [[CrossRef](#)]
25. Haghverdi, A.; Washington-Allen, R.A.; Leib, B.G. Prediction of cotton lint yield from phenology of crop indices using artificial neural networks. *Comput. Electron. Agric.* **2018**, *152*, 186–197. [[CrossRef](#)]
26. De Petris, S.; Berretti, R.; Sarvia, F.; Mondino, E.C.B. Precision arboriculture: A new approach to tree risk management based on geomatics tools. *Remote Sens. Agric. Ecosyst. Hydrol.* **2019**, *219*, 11149, 111491G. [[CrossRef](#)]
27. Orusa, T.; Mondino, E.B. Landsat 8 thermal data to support urban management and planning in the climate change era: A case study in Torino area, NW Italy. In *Remote Sensing Technologies and Applications in Urban Environments IV*; SPIE-Intl Soc Optical Eng.: Bellingham, WA, USA, 2019; Volume 11157, p. 111570O.
28. De Petris, S.; Sarvia, F.; Borgogno-Mondino, E. RPAS-based photogrammetry to support tree stability assessment: Longing for precision arboriculture. *Urban For. Urban Green.* **2020**, *55*, 126862. [[CrossRef](#)]
29. De Petris, S.; Sarvia, F.; Borgogno-Mondino, E. A New Index for Assessing Tree Vigour Decline Based on Sentinel-2 Multi-temporal Data. *Appl. Tree Failure Risk Manag. Remote Sens. Letters* **2020**. [[CrossRef](#)]
30. Sarvia, F.; de Petris, S.; Borgogno-Mondino, E. Multi-scale remote sensing to support insurance policies in agriculture: From mid-term to instantaneous deductions. *GISci. Remote Sens.* **2020**, *57*, 770–784.
31. Borgogno-Mondino, E.; Sarvia, F.; Gomasasca, M.A. Supporting Insurance Strategies in Agriculture by Remote Sensing: A Possible Approach at Regional Level. In *Proceedings of the Lecture Notes in Computer Science*; Springer Science and Business Media LLC: Berlin/Heidelberg, Germany, 2019; pp. 186–199.
32. Sarvia, F.; de Petris, S.; Mondino, E.C.B. Remotely sensed data to support insurance strategies in agriculture. In *Remote Sensing for Agriculture, Ecosystems, and Hydrology XXI*; SPIE-Intl Soc Optical Eng.: Bellingham, WA, USA, 2019; Volume 11149, p. 111491H.
33. Sarvia, F.; de Petris, S.; Borgogno-Mondino, E. A Methodological Proposal to Support Estimation of Damages from Hailstorms Based on Copernicus Sentinel 2 Data Time Series. In *Proceedings of the Lecture Notes in Computer Science*; Springer Science and Business Media LLC: Berlin/Heidelberg, Germany, 2020; pp. 737–751.
34. Chen, J.; Jönsson, P.; Tamura, M.; Gu, Z.; Matsushita, B.; Eklundh, L. A simple method for reconstructing a high-quality NDVI time-series data set based on the Savitzky–Golay filter. *Remote Sens. Environ.* **2004**, *91*, 332–344. [[CrossRef](#)]
35. Corvino, G.; Lessio, A.; Borgogno-Mondino, E. Monitoring Rice Crops in Piemonte (Italy): Towards an Operational Service Based on Free Satellite Data. In *Proceedings of the IGARSS 2018 IEEE International Geoscience and Remote Sensing Symposium, Valencia, Spain, 22–27 July 2018*; Institute of Electrical and Electronics Engineers (IEEE): Piscataway, NJ, USA, 2018; pp. 9070–9073.
36. Mishra, A.; Lu, Y.; Meng, J.; Anderson, A.W.; Ding, Z. Unified framework for anisotropic interpolation and smoothing of diffusion tensor images. *NeuroImage* **2006**, *31*, 1525–1535. [[CrossRef](#)] [[PubMed](#)]
37. Pageot, Y.; Baup, F.; Inglada, J.; Baghdadi, N.; Demarez, V. Detection of Irrigated and Rainfed Crops in Temperate Areas Using Sentinel-1 and Sentinel-2 Time Series. *Remote Sens.* **2020**, *12*, 3044. [[CrossRef](#)]
38. Schreier, J.; Ghazaryan, G.; Dubovyk, O. Crop-specific phenomapping by fusing Landsat and Sentinel data with MODIS time series. *Eur. J. Remote Sens.* **2020**, 1–12. [[CrossRef](#)]
39. Gómez-Giráldez, P.J.; Pérez-Palazón, M.J.; Polo, M.J.; Gonzalez-Dugo, M. Monitoring Grass Phenology and Hydrological Dynamics of an Oak–Grass Savanna Ecosystem Using Sentinel-2 and Terrestrial Photography. *Remote Sens.* **2020**, *12*, 600. [[CrossRef](#)]
40. Veloso, A.; Mermoz, S.; Bouvet, A.; Le Toan, T.; Planells, M.; Dejoux, J.-F.; Ceschia, E. Understanding the temporal behavior of crops using Sentinel-1 and Sentinel-2-like data for agricultural applications. *Remote Sens. Environ.* **2017**, *199*, 415–426. [[CrossRef](#)]
41. Vajsová, B.; Fasbender, D.; Wirthardt, C.; Lemajic, S.; Devos, W. Assessing Spatial Limits of Sentinel-2 Data on Arable Crops in the Context of Checks by Monitoring. *Remote Sens.* **2020**, *12*, 2195. [[CrossRef](#)]
42. Gomasasca, M.A.; Tornato, A.; Spizzichino, D.; Valentini, E.; Taramelli, A.; Satalino, G.; Vincini, M.; Boschetti, M.; Colombo, R.; Rossi, L.; et al. Sentinel for Applications in Agriculture. *ISPRS Int. Arch. Photogramm. Remote Sens. Spat. Inf. Sci.* **2019**, 91–98. [[CrossRef](#)]
43. Conrad, O.; Bechtel, B.; Bock, M.; Dietrich, H.; Fischer, E.; Gerlitz, L.; Wehberg, J.; Wichmann, V.; Böhner, J. System for automated geoscientific analyses (SAGA) v. 2.1. 4. *Geosci. Model Dev. Discuss.* **2015**, *8*. [[CrossRef](#)]
44. Forman, R.T.T. Some general principles of landscape and regional ecology. *Landsc. Ecol.* **1995**, *10*, 133–142. [[CrossRef](#)]
45. Jog, S.; Dixit, M. Supervised classification of satellite images. In *Proceedings of the 2016 Conference on Advances in Signal Processing (CASP), Pune, India, 9–11 June 2016*; Institute of Electrical and Electronics Engineers (IEEE): Piscataway, NJ, USA, 2016; pp. 93–98.
46. Perumal, K.; Bhaskaran, R. Supervised classification performance of multispectral images. *arXiv* **2010**, arXiv:1002.4046.
47. Keuchel, J.; Naumann, S.; Heiler, M.; Siegmund, A. Automatic land cover analysis for Tenerife by supervised classification using remotely sensed data. *Remote Sens. Environ.* **2003**, *86*, 530–541. [[CrossRef](#)]
48. Fischer, R.A.; Santiveri, F.; Vidal, I.R. Crop rotation, tillage and crop residue management for wheat and maize in the sub-humid tropical highlands: I. Wheat and legume performance. *Field Crops Res.* **2002**, *79*, 107–122. [[CrossRef](#)]
49. Reeves, T.; Ellington, A.; Brooke, H. Effects of lupin-wheat rotations on soil fertility, crop disease and crop yields. *Aust. J. Exp. Agric.* **1984**, *24*, 595–600. [[CrossRef](#)]

50. Richards, J.A.; Richards, J.A. *Remote Sensing Digital Image Analysis*; Springer: Berlin, Germany, 1999; Volume 3, pp. 10–38.
51. Hasmadi, M.; Pakhriazad, H.Z.; Shahrin, M.F. Evaluating supervised and unsupervised techniques for land cover mapping using remote sensing data. *Geogr. Malays. J. Soc. Space* **2009**, *5*, 1–10.
52. South, S.; Qi, J.; Lusch, D.P. Optimal classification methods for mapping agricultural tillage practices. *Remote Sens. Environ.* **2004**, *91*, 90–97. [[CrossRef](#)]
53. Wacker, A.G.; Landgrebe, D.A. *Minimum Distance Classification in Remote Sensing*; LARS Technical Reports for Purdue University: West Lafayette, IN, USA, 1972; p. 25.
54. Hodgson, M.E. Reducing the computational requirements of the minimum-distance classifier. *Remote Sens. Environ.* **1988**, *25*, 117–128. [[CrossRef](#)]
55. Breiman, L. Bagging predictors. *Mach. Learn.* **1996**, *24*, 123–140. [[CrossRef](#)]
56. Liaw, A.; Wiener, M. Classification and regression by Random Forest. *R News* **2002**, *2*, 18–22.
57. Ok, A.O.; Akar, O.; Gungor, O. Evaluation of random forest method for agricultural crop classification. *Eur. J. Remote Sens.* **2012**, *45*, 421–432. [[CrossRef](#)]
58. Sonobe, R.; Tani, H.; Wang, X.; Kobayashi, N.; Shimamura, H. Random forest classification of crop type using multi-temporal TerraSAR-X dual-polarimetric data. *Remote Sens. Lett.* **2014**, *5*, 157–164. [[CrossRef](#)]
59. Pal, M. Random forest classifier for remote sensing classification. *Int. J. Remote Sens.* **2005**, *26*, 217–222. [[CrossRef](#)]
60. Hay, A. The derivation of global estimates from a confusion matrix. *Int. J. Remote Sens.* **1988**, *9*, 1395–1398. [[CrossRef](#)]
61. Konduri, V.S.; Kumar, J.; Hargrove, W.W.; Hoffman, F.M.; Ganguly, A.R. Mapping crops within the growing season across the United States. *Remote Sens. Environ.* **2020**, *251*, 112048. [[CrossRef](#)]
62. Belgiu, M.; Csillik, O. Sentinel-2 cropland mapping using pixel-based and object-based time-weighted dynamic time warping analysis. *Remote Sens. Environ.* **2018**, *204*, 509–523. [[CrossRef](#)]
63. Palchowdhuri, Y.; Valcarce-Diñeiro, R.; King, P.; Sanabria-Soto, M. Classification of multi-temporal spectral indices for crop type mapping: A case study in Coalville, UK. *J. Agric. Sci.* **2018**, *156*, 24–36. [[CrossRef](#)]
64. Jiang, Y.; Lu, Z.; Li, S.; Lei, Y.; Chu, Q.; Yin, X.; Chen, F. Large-Scale and High-Resolution Crop Mapping in China Using Sentinel-2 Satellite Imagery. *Agriculture* **2020**, *10*, 433. [[CrossRef](#)]